Membrane topology of the C-terminal half of the neuronal, glial, and bacterial glutamate transporter family

Slotboom, DJ; Lolkema, JS; Konings, WN

Published in:
The Journal of Biological Chemistry

DOI:
10.1074/jbc.271.49.31317

THE JOURNAL OF BIOLOGICAL CHEMISTRY
Vol. 271, No. 49, Issue of December 6, pp. 31317–31321, 1996

Printed in U.S.A.

Membrane Topology of the C-terminal Half of the Neuronal, Glial, and Bacterial Glutamate Transporter Family*

(Received for publication, September 12, 1996, and in revised form, October 17, 1996)

Dirk Jan Slotboom, Juke S. Lolkema‡, and Wil N. Konings

From the Department of Microbiology, Groningen Biomolecular Sciences and Biotechnology Institute, University of Groningen, Kerklaan 30, 9751 NN Haren, The Netherlands

Secondary glutamate transporters in neuronal and glial cells in the mammalian central nervous system remove the excitatory neurotransmitter glutamate from the synaptic cleft and prevent the extracellular glutamate concentration to rise above neurotoxic levels. Secondary structure prediction algorithms predict 6 transmembrane helices in the first half of the transporters but fail in the C-terminal half where no clear helix-loop-helix motif is resolved in the hydropathy profile of the primary sequences. A number of previous studies have emphasized the importance of the C-terminal half of the molecules for the function. Here we determine the membrane topology of the C-terminal half of the glutamate transporters by applying the *phoA* gene fusion technique to the homologous bacterial glutamate transporter of *Bacillus stearothermophilus*. High sequence conservation and very similar hydropathy profiles in the C-terminal half warrant a similar folding as in the glutamate transporters of the mammalian central nervous system. The C-terminal half contains four putative transmembrane helices. The strong hydrophobic moment and substitution moment of the most C-terminal helix X that point to opposite faces of the helix suggest that the helix faces the lipid environment with its least conserved, hydrophobic face and the interior of the protein with its well conserved, hydrophilic face. Residues that were shown before to be critical for function cluster in helix X and VII.

Glutamate is the predominant excitatory neurotransmitter in the mammalian central nervous system. High affinity Na^+- and K^+-dependent glutamate transporters in presynaptic nerve terminals and glial cells terminate the transmission by removing the neurotransmitter from the synaptic cleft and are essential to keep the extracellular concentration of glutamate below neurotoxic levels (1). Impaired glutamate uptake has been implicated with neurodegenerative diseases (2). Glutamate transporters from different mammalian sources have been cloned and sequenced and were characterized electrophysiologically and biochemically (15–18), but the understanding of the molecular basis of transport is hampered by a lack of structural information on the transporters.

* This work was supported by the Ministry of Economic Affairs, the Ministry of Education, Culture and Sciences, and the Ministry of Agriculture, Nature Management and Fishery in the framework of an industrial relevant research program of the Netherlands Association of Biotechnology Centres in The Netherlands (ABON). The costs of publication of this article were defrayed in part by the payment of page charges. This article must therefore be hereby marked "*advertisement*" in accordance with 18 U.S.C. Section 1734 solely to indicate this fact.

‡ To whom correspondence should be addressed: Dept. of Microbiology, University of Groningen, Kerklaan 30, 9751 NN Haren, The Netherlands. Tel.: 31-50-363-2155; Fax: 31-50-363-2154; E-mail: j.s.lolkema@biol.rug.nl.

The neuronal and glial glutamate transporters belong to a family of homologous transporter proteins in which also glutamate transporters from prokaryotic origin are found. Alignment of the primary sequences in the family reveals about 30% sequence identity between the prokaryotic and eukaryotic members. In spite of this low degree of sequence conservation, the hydropathy profiles of the transporters are well conserved, suggesting that their membrane topology and global structure is the same (3). Several models have been proposed for the membrane topology of the individual members of the family. These models univocally predict six transmembrane helices in the N-terminal half of the proteins, but there is no consensus about the topology of the C-terminal half. Models with zero, two, and four helices in this part of the protein have been proposed (3, 15–17). This is unfortunate because in particular the C-terminal half of the glutamate carriers is the best conserved part of the proteins and has been postulated to constitute the translocation pathway (4). Evidence supporting the hypothesis comes from mutagenesis studies with the glutamate transporters GLAST and GLT-1 from rat brain by which several residues in the C-terminal half were identified that are critical for the function of the transporters (5, 6). Furthermore, the binding site of dihydrokainic acid, a glutamate analogue, has been located in the C-terminal half of the human excitatory glutamate transporter EAAT2 (7).

In this study the membrane topology of the C-terminal half of one member of the family of glutamate transporters, GltT of *Bacillus stearothermophilus*, is determined using the well established *phoA*-gene fusion approach (22). A total of 19 GltT-PhoA fusion proteins with fusion sites at approximately every sixth residue in the primary sequence of the C-terminal half of GltT were constructed. Clusters of fusion proteins with low and high alkaline phosphatase activity alternate along the primary sequence of GltT, indicating the presence of 4 transmembrane helices in addition to the 6 predicted helices in the N-terminal half.

EXPERIMENTAL PROCEDURES

Bacterial Strains and Growth Conditions—Escherichia coli strain JM101 expressing the GltT derivatives was grown in Luria Broth (LB) medium containing carbenicillin at a concentration of 100 μg/ml at 37 °C. The constructs were expressed in the absence of isopropyl-1-thio-β-D-galactopyranoside. The cells were screened for alkaline phosphatase activity by plating on LB agar plates containing 40 μg/ml 5-bromo-4-chloroindolyl phosphate (XP).[1]

Construction of gltT-phoA Gene Fusions—Standard recombinant DNA procedures were used essentially as described by Sambrook *et al.* (8). Plasmid pGltThis codes for the GltT protein with 6 additional histidine residues (His-tag) at the N terminus and is routinely used as the expression vector for the purification of the protein (9). pGltThis contains a unique *Hin*dIII restriction site in the first half of the *gltT* gene and a unique *Xba*I site downstream of the gene. The polymerase chain reaction technique was used to amplify fragments of the *gltT* gene

[1] The abbreviation used is: XP, 5-bromo-4-chloroindolyl phosphate.

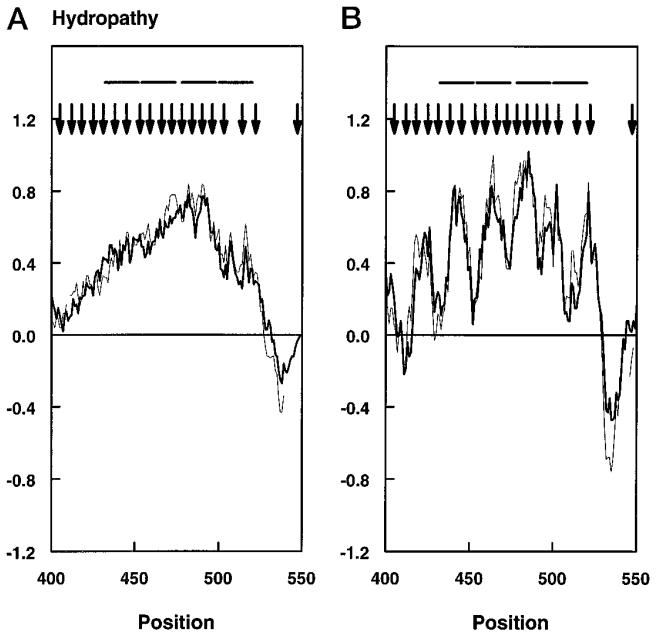

FIG. 1. **Hydropathy profile analysis of the C-terminal half of the aligned set of glutamate transporters.** Hydropathy profiles were calculated using a window of 21 (*A*) and 11 (*B*) residues. *Position numbers* refer to the positions in the alignment. *Bold* and *thin lines* indicate average profiles and the GltT profiles, respectively. *Arrows* and *bars* indicate the fusion sites in the GltT-PhoA fusions and the membrane spanning helices, respectively.

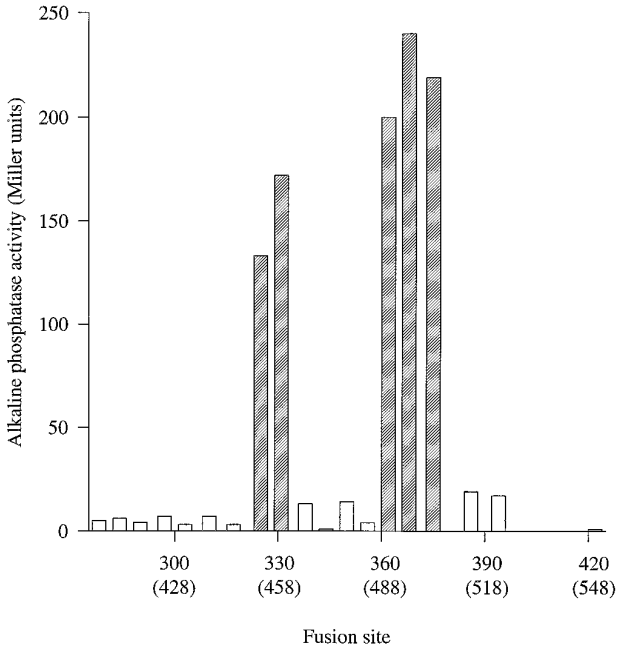

FIG. 2. **Alkaline phosphatase activity of cells expressing GltT-PhoA fusion proteins.** The average value of three measurements is shown. The *numbers* indicating the fusion sites refer to the residue numbers in the sequence of GltT, whereas the positions in the multiple sequence alignment (as in Fig. 1) are shown in *parentheses. Hatched* and *open bars* indicate cells expressing hybrid proteins that appear as blue and white colonies on indicator plates containing the chromogenic substrate for alkaline phosphatase 5-bromo-4-chloro-5-indolyl phosphate, respectively.

from the *Hin*dIII site to the desired fusion site where a *Nco*I site was introduced in the fragment. The ATG bases of the *Nco*I sites were in frame with the coding sequence. The polymerase chain reaction products were restricted with *Hin*dIII and *Nco*I and cloned in vector pSK*phoA* that contains the coding sequence for the mature form of alkaline phosphatase starting with a *Nco*I site and flanked by unique *Hin*dIII (upstream) and *Xba*I (downstream) restriction sites (11). In the resulting vector, the *phoA* gene is fused to the *gltT* fragments. Finally, the *Hin*dIII-*Xba*I fragments of these plasmids were cloned back into pGltThis digested with the same enzymes which results in the complete *gltT-phoA* gene fusions. The nucleotide sequences of the amplified *gltT* fragments were confirmed on a Vistra 725 automated Sequencer.

Alkaline Phosphatase Activities and Immunoblot Analysis—Alkaline phosphatase activities of exponentially growing cells were quantified by measuring the rate of *p*-nitrophenyl phosphate hydrolysis essentially as described by Michaelis *et al.* (10) with minor modifications according to Van Geest and Lolkema (11). Immunoblot analysis of exponentially growing cells expressing GltT-PhoA fusion proteins was performed as described by Van Geest and Lolkema (11) using a monoclonal antibody directed against alkaline phosphatase. Antibodies were visualized using the Western light chemiluminescence detection kit (Tropix).

Sequence Analysis—A selection of 7 representative homologous glutamate transporters were included in the analysis. All other homologous glutamate transporters in the data bases share at least 90% sequence identity with one of these sequences. The family includes GLT1 of *Rattus norvegicus* (EMBL Databank accession number X67857) (15), GLAST of *R. norvegicus* (X63744) (16), EAAC1 of *Oryctolagus cuniculus* (L12411) (17), EAAT4 of *Homo sapiens* (U18244) (18), GltP of *E. coli* (M84805) (19), GltP of *Bacillus subtilis* (U15147) (20), and GltT of *B. stearothermophilus* (M86508) (21). Multiple sequence alignments were performed using the program ClustalV (12). Hydropathy profiles were calculated using the normalized hydrophobicity scale of Kyte (13). Profiles of the hydrophobic moment and substitution moment with α-helical periodicity were calculated using the method of Eisenberg (13) with the normalized hydrophobicity scale of Kyte and the substitution table of Donnelly *et al.* (14), respectively.

RESULTS

Hydropathy Profile Analysis—Fig. 1 shows the average hydropathy profile of the aligned primary sequences of the C-terminal half of the family of neuronal, glial, and bacterial glutamate transporters. The region between position 410 and 530 is present in all sequences and does not contain any gaps in the alignment. The profile reveals one large hydrophobic region with very little structure when a window size of 21 residues is used which makes it difficult to assign transmembrane segments (Fig. 1*A*). The lack of structure is not a consequence of the averaging of the different sequences in the family. Reducing the window size to 11 residues reveals a "fine structure" in the profile that is extremely well conserved throughout the family. The profile of the individual GltT sequence that is indicated separately in Fig. 1*B* almost coincides with the average profile. The strong conservation of the hydropathy profiles throughout the family indicates that the membrane topology of all members is the same and that the topology of any member can be used as a model for the others.

GltT-PhoA Fusion Proteins—The glutamate transporter GltT of *B. stearothermophilus* was selected as the model to determine the membrane topology of the C-terminal half of the glutamate transporter family. The GltT protein can be expressed in *E. coli* in a functional form (9, 21), allowing the well documented alkaline phosphatase (*phoA*)-gene fusion technique to determine the disposition of the polypeptide chain in the membrane (22). Alkaline phosphatase was fused to C-terminally truncated GltT molecules at the 19 sites indicated by the *arrows* in Fig. 1. The spacing between the sites is approximately 6 residues.

Expression of the GltT-PhoA fusion proteins in *E. coli* resulted in two different phenotypes when the cells were plated on LB agar containing the chromogenic substrate for alkaline phosphatase. The cells grew either as blue or white colonies, indicative of high and low alkaline phosphatase activity, respectively. The activity was quantified by measuring the rate of hydrolysis of *p*-nitrophenyl phosphate catalyzed by the cells expressing the different fusion proteins in suspension. Cells with a blue phenotype on XP plates showed at least a 10-fold higher alkaline phosphatase activity than cells with a white

phenotype (Fig. 2). Expression of the GltT-PhoA fusion proteins was demonstrated by Western blot analysis using a monoclonal antibody against PhoA (Fig. 3). The experiments were carried out with the same batches of cells that were used to determine the PhoA activities of the fusion proteins. *E. coli* JM101 expressing wild type GltT and grown in rich medium does not express chromosomally encoded alkaline phosphatase as is evident from the lack of signal in *lanes A14* and *B1*. In all cases, the full-length GltT-PhoA fusion protein is observed increasing in size from about 70 kDa for the most N-terminal fusion at residue 278 to 84 kDa for the C-terminal fusion. The lower molecular weight bands represent breakdown products. There is no clear correlation between the blue and white phenotype of the cells (Fig. 2), and the level of expression or the stability of the fusion proteins. This is in contrast to other *phoA*-gene fusion studies where PhoA fusion proteins conferring low alkaline phosphatase activity were rapidly degraded while fusion proteins conferring high activity were stable (*e.g.* Refs. 11 and 23). Here, we conclude that the activity of the different fusion proteins correlates with low specific activity rather than low expression levels.

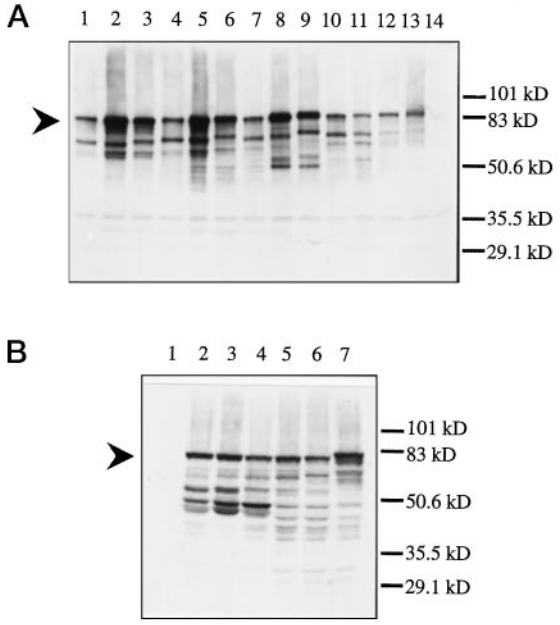

FIG. 3. **Western blot analysis of cells expressing GltT-PhoA fusions.** Cells expressing fusion proteins were run on a 10% SDS-polyacrylamide gel and detected using a monoclonal antibody directed against PhoA. *A*, *lanes 1–13*, cells expressing GltT with PhoA fused at residues 278, 284, 290, 297, 303, 310, 317, 325, 331, 338, 344, 350, and 356, respectively; *lane 14*, cells expressing wild type GltT. *B*, *lanes 2–7*, cells expressing GltT with PhoA fused at residues 362, 368, 375, 386, 394, and 422, respectively; *lane 1*, cells expressing wild type GltT. The *arrow* indicates the fusion proteins.

The Topology Model—The fusion sites in the GltT-PhoA fusion proteins resulting in low and high PhoA activities group into three and two clusters, respectively, that alternate along the primary sequence of GltT (Fig. 2). Since PhoA is only active when translocated to the periplasm, the fusion sites in the proteins with high PhoA activities are at the periplasmic side of the membrane, whereas the fusion sites in the proteins with low PhoA activities are at the cytoplasmic side of the membrane (22). This indicates the presence of four membrane spanning segments in the C-terminal half of the glutamate carriers. Detailed studies with the lactose permease, LacY, and the melibiose carrier, MelB, from *E. coli* have demonstrated that the N-terminal half of an outgoing transmembrane helix is sufficient to export the PhoA moiety fused to a membrane protein while the N-terminal half of an ingoing transmembrane helix is sufficient to prevent the export of the PhoA moiety to the periplasm (23, 24). This suggests that the middle of a transmembrane helix is located in between fusion sites resulting in high and low alkaline phosphatase activity. The alkaline phosphatase activity profile of the fusion sites in GltT shows remarkably sharp transitions between sites that are only 6 to 10 residues apart which localizes the middle of the transmembrane segments in between residues 317 and 325, 331 and 338, 356 and 362, and between 375 and 386. This together with the

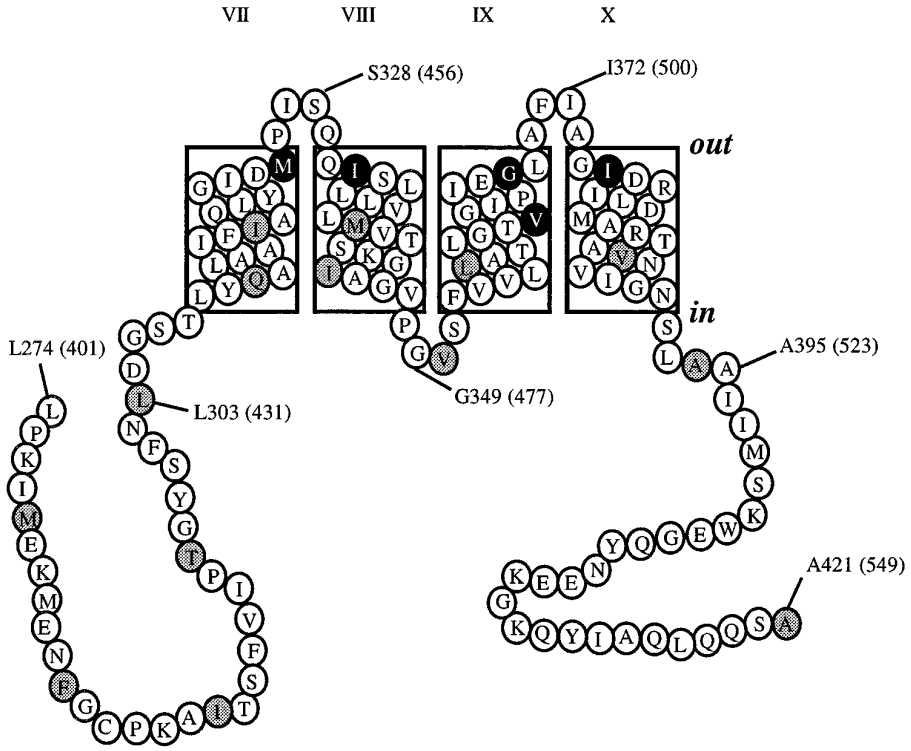

FIG. 4. **Model for the membrane topology of the C-terminal half of the glutamate transporter family.** The sequence of GltT is shown, and *residue numbers* refer to the GltT sequence while the positions in the multiple sequence alignment are shown in *parentheses*. The putative membrane spanning helices VII through X are indicated in *boxes*. The fusion sites in the GltT-PhoA hybrids with high and low alkaline phosphatase activity are shown in *black* and *gray*, respectively.

assumption that a transmembrane segment requires about 20 residues to traverse the membrane results in the topology model for the C-terminal half of GltT presented in Fig. 4.

DISCUSSION

The membrane topology of the C-terminal half of the neuronal, glial, and bacterial glutamate transporter family was determined with the *phoA*-gene fusion technique using GltT of *B. stearothermophilus* as the representative model. The results reveal the presence of four membrane spanning segments, which, taken together with the 6 membrane helices that have been predicted in the N-terminal half of the protein (3), results in a total of 10 transmembrane helices in the glutamate transporters. The folding model for the C-terminal half presented in Fig. 4 is in agreement with trypsin digestion studies performed with membrane vesicles from rat brain containing GLT-1 (25). These studies showed that an antibody epitope near the C terminus of the transporter as well as an epitope between residues 372 and 386 in the sequence of GLT-1, corresponding to residues 278 to 292 in the sequence of GltT (Fig. 4), are located at the cytoplasmic side of the membrane.

The location of the four putative transmembrane helices is indicated in the hydropathy profiles of Fig. 1. The first three helices (helices VII, VIII, and IX) roughly coincide with peaks in the hydropathy profile when a small window size is used indicating that at least the core of these helices is hydrophobic (Fig. 1*B*). However, the membrane spanning segment that is located closest to the C terminus of the protein (helix X) is not very hydrophobic. It contains several well conserved charged and polar residues that have to be accommodated in the apolar core of the membrane. To provide more insight in the structure of this segment, the periodicity profile approach of Eisenberg was used (13, 26). Putative transmembrane helix X exhibits exceptionally strong hydrophobic and substitution moments with α-helical periodicity (Fig. 5, *A* and *B*). The hydrophobic moment is large compared to highly amphipatic helices in known structures, *e.g.* the peptide melittin has a hydrophobic moment of 0.4/residue (13) which compares to 0.49/residue for helix X on the same hydrophobicity scale. The hydrophobic moment is extremely well conserved throughout the family and indicates a helical structure that is hydrophobic at one face and hydrophilic at the opposite face. Similarly, the large substitution moment follows from clustering of conserved residues at one face of the helix. In the crystal structure of the bacterial reaction center, the least conserved residues of a transmembrane helix tend to face the lipids whereas the more conserved residues are buried in the protein interior (26). A helical wheel representation of putative transmembrane helix X shows that the hydrophobic and substitution moments point to opposite faces of the helix (Fig. 5*C*). The least conserved face of the helix is hydrophobic whereas the conserved residues are at the opposite hydrophilic side. Consequently, the transmembrane helix could have a lipid-exposed hydrophobic face and a hydrophilic face of conserved residues that interact with hydrophilic residues on adjacent transmembrane segments. Polar and charged residues are not expected in the hydrophobic core of the membrane unless they are essential for the function of the protein. Indeed, two conserved hydrophilic residues in transmembrane helix X have been shown to be crucial for transporter function as evidenced by the complete loss of transport activity when Asp-470 (position 504 in the multiple sequence alignment of Fig. 5*C*) in GLT1 is substituted for Asn, Gly, or Glu and Arg-479 (position 511) in GLAST is substituted for Thr (5, 6). The hydrophilic residues of amphipatic helix X form a hydrophilic surface that spans the entire apolar core of the membrane and can provide the pathway for the translocation of glutamate and/or the co-ions through the protein.

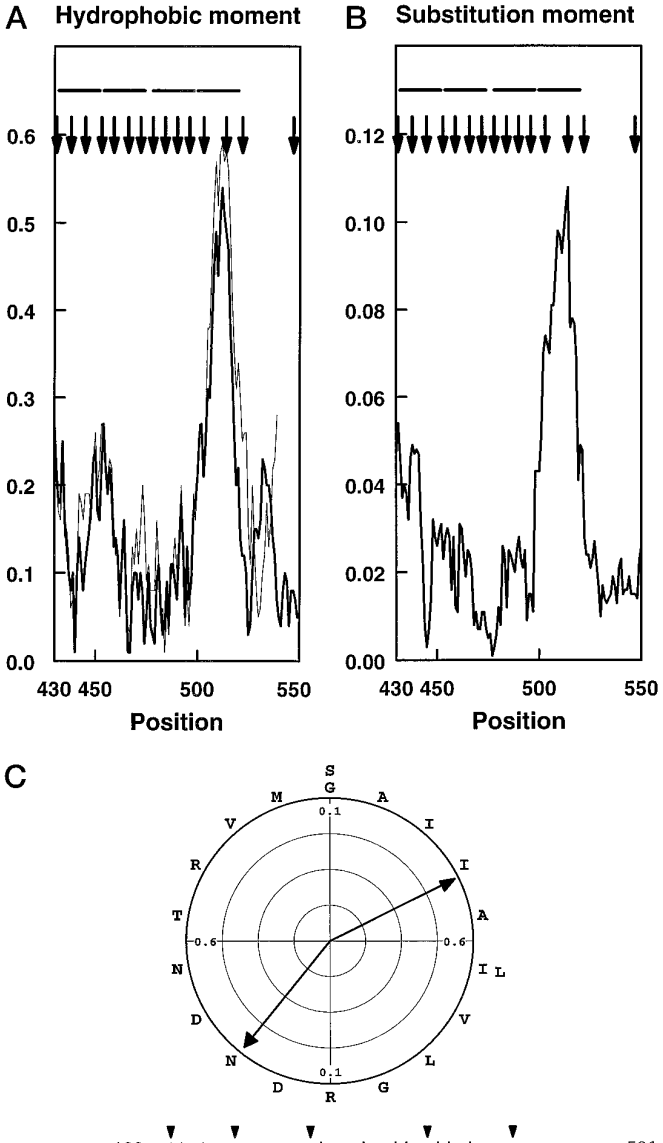


```
          489 ~**~* ~ ~~ ~  ~*  ~*  **  ** * ~   ~~      531
GLT1 rn   455 AVGLPTEDISLLVAVDWLLDRMRTSVNVVGDSFGAGIVVHLSK 497
EAAC1 oc  425 AVGLPAEDVTLIIAVDWLLDRFRTVVNVLGDAFGTGIVEKLSK 467
GLAST rn  457 SVGLPTDDITLIIAVDWFLDRLRTTTNVLGDSLGAGIVEHLSR 499
EAAT4 hs  482 SVGLPTEDITLIIAVDWFLDRLRTMTNVLGDSIGAAVIEHLSQ 524
GltP ec   371 SVGIPLEGLAFIAGVDRILDMARTALNVVGNALAVLVIAKWEH 413
GltT bst  361 TVGIPIEGLAFIAGIDRILDMARTAVNVIGNSLAAIIMSKWEG 403
GltP bs   355 AVGLPAEGVAIIAGVDRVMDMARTGVNVPGHAIACIVVSKWEK 397
```

FIG. 5. **Periodicity profile analysis of the C-terminal half of the glutamate transporters family.** Profiles of the hydrophobic moment (*A*) and substitution moment (*B*) with α-helical periodicity using a window of 21 residues. The moments are given per residue. *Position numbers* refer to the positions in the multiple sequence alignment. *Bold* and *thin lines* indicate average profiles and the GltT profiles, respectively. *Arrows* and *bars* indicate the fusion sites in the GltT-PhoA fusions and the membrane spanning helices, respectively. *C*, helical wheel representation of the hydrophobic moment and substitution moment of putative helix X. The hydrophobic moment averaged over the family and given per residue (*right arrow*; scale 0.6), and the substitution moment per residue (*left arrow*; scale 0.1) were calculated for the stretches shown in *bold* in the alignment below. The sequence of GltT is shown on the *wheel*. The *numbers in the top line* of the multiple sequence alignment refer to the position numbers in the alignment, and the symbols ~ and * indicate similar and identical residues, respectively. The residue numbering of the individual sequences is shown on each side of the sequences. The *triangles* indicate the fusion sites in the GltT-PhoA fusion proteins.

Three other polar or charged residues that have been shown to be important for the function of the glutamate transporters from rat brain are located in helix VII. Asp-398 in GLT-1 (corresponding to Asp-304 in the sequence of GltT in Fig. 4) and

Tyr-405 in GLAST (Tyr-309 in GltT) are essential for transport of glutamate whereas mutation of the nonconserved residue Glu-404 in GLT-1 (Gln-310 in GltT) changes the substrate specificity of the transporter (5, 6). Helix VII is also part of the stretch that contains the binding site of the glutamate analogue dihydrokainic acid in the human excitatory glutamate transporter EAAT2 (7). Therefore, helices VII and X may provide an important part of the binding site and translocation path in the glutamate carriers.

REFERENCES

1. Kanner, B. I. (1993) *FEBS Lett.* **325,** 95–99
2. Rothstein, J. D., Jin, L., Dykes-Hoberg, M., and Kuncl, R. W. (1993) *Proc. Natl. Acad. Sci. U. S. A.* **90,** 6591–6595
3. Kanai, Y., Smith, C. P., and Hediger, M. A. (1993) *FASEB J.* **7,** 1450–1459
4. Kanai, Y., Nussberger, S., Romero, M. F., Boron, W. F., Hebert, S. C., and Hediger, M. A. (1995) *J. Biol. Chem.* **270,** 16561–16568
5. Pines, G., Zhang, Y., and Kanner, B. I. (1995) *J. Biol. Chem.* **270,** 17093–17097
6. Conradt, M., and Stoffel, W. (1995) *J. Biol. Chem.* **270,** 25207–25212
7. Vandenberg, R. J., Arriza, J. L., Amara, S. G., and Kavanaugh, M. P. (1995) *J. Biol. Chem.* **270,** 17668–17671
8. Sambrook, J., Fritch, E. F., and Maniatis, T. (1989) *Molecular Cloning: A Laboratory Manual*, Cold Spring Harbor Laboratory Press, Cold Spring Harbor, NY
9. Gaillard, I., Slotboom, D. J., Knol, J., Lolkema, J., and Konings, W. N. (1996) *Biochemistry* **35,** 6150–6156
10. Michaelis, S., Hunt, J., and Beckwith, J. (1986) *J. Bacteriol.* **167,** 160–167
11. Van Geest, M., and Lolkema, J. S. (1996) *J. Biol. Chem.* **271,** 25582–25589
12. Higgins, D., and Sharp, P. (1988) *Gene* (*Amst.*) **73,** 237–244
13. Eisenberg, D. (1984) *Annu. Rev. Biochem.* **53,** 595–623
14. Donnelly, D., Overington, J. P., Ruffle, S. V., Nugent, J. H. A., and Blundell, T. (1993) *Protein Sci.* **2,** 55–70
15. Pines, G., Danbolt, N. C., Bjøras, M., Zhang, Y., Bendahan, A., Eide, L., Koepsel, H., Storm-Mathisen, J., Seeberg, E., and Kanner, B. I. (1992) *Nature* **360,** 464–467
16. Storck, T., Schulte, S., Hofman, K., and Stoffel, W. (1992) *Proc. Natl. Acad. Sci. U. S. A.* **89,** 10955–10959
17. Kanai, Y., and Hediger, M. A. (1992) *Nature* **360,** 367–371
18. Fairman, W. A., Vandenberg, R. J., Arriza, J. L., Kavanaugh, M., and Amara, S. G.(1995) *Nature* **375,** 599–603
19. Tolner, B., Poolman, B., Wallace, B., and Konings, W. N. (1992) *J. Bacteriol.* **174,** 2391–2393
20. Tolner, B., Ubbink-Kok, T., Poolman, B., and Konings, W. N. (1995) *J. Bacteriol.* **177,** 2863–2869
21. Tolner, B., Poolman, B., and Konings, W. N. (1992) *Mol. Microbiol.* **6,** 2845–2856
22. Manoil, C., and Beckwith, J. (1986) *Science* **233,** 1403–1408
23. Pourcher, T., Bibi, E., Kaback, H. R., and Leblanc, G. (1996) *Biochemistry* **35,** 4161–4168
24. Calamia, T., and Manoil, C. (1990) *Proc. Natl. Acad. Sci. U. S. A.* **87,** 4937–4941
25. Grunewald, M., and Kanner, B. I. (1995) *J. Biol. Chem.* **270,** 17017–17024
26. Rees, D. C., DeAntonio, L., and Eisenberg, D. (1989) *Science* **245,** 510–513